

Reactivity and Gas-phase Acidity Determinations of Small Peptide Ions Consisting of 11 to 14 Amino Acid Residues

Scott R. Carr and Carolyn J. Cassady

Department of Chemistry, Miami University, Oxford, Ohio 45056, USA

Small peptides ions consisting of a comparable number of amino acid residues but varying in composition and sequence were allowed to undergo gas-phase deprotonation reactions. These multiply protonated ions were generated by electrospray ionization and analyzed in a Fourier transform ion cyclotron resonance (FT-ICR) mass spectrometer. The peptides studied contain 11–14 amino acid residues and included adrenocorticotrophic hormone (ACTH) fragment (11–24), fibrinopeptide B (human), gastrin I fragment (1–13) (human), renin substrate tetradecapeptide (horse), somatostatin, substance P and tyrosine protein kinase. Rate constants were determined for the deprotonation reactions of the peptide ions with a series of reference compounds of known gas-phase basicities ranging from 190.0 to 232.6 kcal mol⁻¹. From these values, apparent gas-phase acidities (GA_{app}) were assigned to $[M + nH]^{n+}$ ($n \geq 2$), of each peptide. All of the multiply charged peptide ions were sequentially deprotonated to the +1 charge state by ion–molecule reactions. The GA_{app} s ranged from 193.3 kcal mol⁻¹ (for $[M + 4H]^{4+}$ of renin substrate, the ion most readily deprotonated) to >232.6 kcal mol⁻¹ (for $[M + 2H]^{2+}$ of ACTH (11–24), the ion most difficult to deprotonate). The proximity of intrinsically basic sites (and therefore potential protonation sites) has an effect on the observed deprotonation rates. Ions experiencing Coulomb repulsion resulting from adjacent protonation sites often show more facile deprotonation. However, the intrinsic basicity of a protonation site also plays a role in determining the ease of deprotonation. As a result, some lower charge state peptide ions deprotonate more readily than other peptides with higher charges but with more basic protonation sites. In addition, conformation and the influence of intramolecular hydrogen bonding may affect the reactivity of some peptide ions. Also observed was non-linear kinetic behavior that indicates multiple isomers at certain charge states for some peptides, e.g. $[M + nH]^{n+}$, ($n = 2$ and 3) for ACTH 11–24 and $[M + 3H]^{3+}$ for somatostatin. © 1997 by John Wiley & Sons, Ltd.

J. Mass Spectrom. **32**, 959–967 (1997)

No. of Figs: 4 No. of Tables: 4 No. of Refs: 48

KEYWORDS: Fourier transform ion cyclotron resonance mass spectrometry; Fourier transform mass spectrometry; peptides; electrospray ionization; ion–molecule reactions; apparent gas-phase acidity

INTRODUCTION

Electrospray ionization (ESI) has greatly facilitated the analysis of biomolecules in the gas phase. It is now common to study the gas-phase reaction chemistry of large multiply charged ions produced via this ionization process. For example, hydrogen–deuterium exchange reactions,^{1,2} ion–ion reactions^{3,4} and ion–molecule proton transfer reactions^{1,5–9} have been performed to probe the characteristics of ESI-generated biomolecular ions.

Protons on multiply charged peptides have been suggested to be located primarily on basic amino acid residues.^{2,10–12} Of the common α -amino acids, three are significantly more basic than the other, namely arginine,

lysine and histidine.^{13–15} In addition, the *N*-terminal amino group is considered a possible protonation site.¹⁰ Proline, glutamine and tryptophan residues have also been suggested as sites of protonation for higher charge state ions.¹⁶ The effects of proton locations on the conformation and reactivity of biomolecules are in an active area of research.^{1,6,7,17–19} Proton transfer properties of biomolecules in solution are important in physiology where the conformation may be vital to a molecule's functioning. Determining the extent and sites of protonation for a biomolecule in the gas phase may provide information that increases the understanding of solution-phase mechanisms.

Several studies have examined the thermodynamic properties of apparent gas-phase acidity (GA_{app}) and basicity (GB_{app}) for multiply charged biomolecules.^{1,6–9,16,20–22} Fenselau and co-workers have determined the GB_{app} s for $[M + H]^+$ of the nonapeptide bradykinin²⁰ and des-Arg⁹-bradykinin²² by a modified kinetic method. Similar studies were performed on $[M + nH]^{n+}$ ($n = 2$ and 3) for the 26 residue peptide melittin.²¹ This group also used kinetic energy release measurements to evaluate the reverse activation

* Correspondence to: C. J. Cassady, Department of Chemistry, Miami University, Oxford, Ohio 45056, USA.

Contract grant sponsor: National Institutes of Health; Contract grant number: RO1-GM51384-O1A1.

Contract grant sponsor: Ohio Board of Regents.

barrier resulting from Coulomb repulsion during deprotonation of multiply charged ions.²⁰ In addition, deprotonation reactions have been used to obtain thermodynamic values for peptide and protein ions. For example, Gross and Williams⁸ measured the GB_{app} for $[M + H]^+$ of the cyclic decapeptide gramicidin S by deprotonation of $[M + 2H]^{2+}$. From the deprotonation data and molecular modeling results, they determined values for Coulomb energy and dielectric polarizability related to this system. Williams and co-workers have also used deprotonation reactions to obtain GB_{app} s for larger protein ions from cytochrome *c*⁹ and lysozyme.⁷ The data obtained in these studies allow the evaluation of likely sites of protonation and the extent of electrostatic interactions, in addition to their effects on structural conformation.

Recently, Zhang and Cassady⁶ used deprotonation reactions with a series of reference compounds to obtain GA_{app} values for $[M + nH]^{n+}$ produced from the small peptide renin substrate ($n = 2-4$) and from larger peptides insulin chain B ($n = 2-5$) and ubiquitin ($n = 4-13$). (The quantity of $GA_{app}([M + nH]^{n+})$ is essentially the same as $GB_{app}([M + (n-1)H]^{(n-1)+})$; GA_{app} has been suggested as a more appropriate term for use with multiply charged ions because it directly relates to the parent ion being deprotonated.²³⁻²⁵) This work suggested that, at a given mass-to-charge ratio, the GA_{app} s of peptide ions agree to within 10 kcal mol⁻¹ (1 kcal = 4.184 kJ) despite large differences in mass and charge. However, the smallest peptide studied, renin substrate, deviated most from this observation, which may indicate that as the number of potential protonation sites decreases intrinsic basicity of the residues becomes more of a factor in deprotonation processes.

The present study focuses on seven multiply charged peptide ions which consist of 11-14 amino acid residues, but vary in composition and sequence. The effects of primary peptide structure on deprotonation reactivity and on charge state production are explored. The GA_{app} value for each charge state produced by ESI was obtained from the deprotonation reaction data.

EXPERIMENTAL

All experiments were performed using an external Analytica of Branford (Branford, CT, USA) ESI source interfaced to a Bruker (Billerica, MA, USA) BioAPEX-47e Fourier transform ion cyclotron resonance (FT-ICR) mass spectrometer. Some experimental details have been described previously.^{1,6} Briefly, solutions of small peptides were prepared in a water-methanol-acetic acid solvent (49.5:49.5:1) in a concentration range of $(1.0-5.0) \times 10^{-5}$ M and were introduced into the ESI source by a syringe pump at a flow rate of 0.8-3.0 μ l min⁻¹. The peptide solutions flowed through a grounded ESI needle and passed into an electric field with a 3-4 kV potential at atmospheric pressure. Heated (180-200 °C) CO₂ was used as a drying gas to facilitate evaporation of the sprayed solutions. The multiply charged peptide ions, $[M + nH]^{n+}$, were transferred to the FT-ICR cell via electrostatic focusing. Owing to five stages of differential pumping, a back-

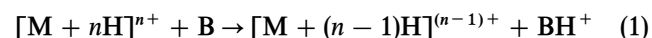
ground pressure in the analyzer region of $\sim 5 \times 10^{-10}$ Torr (1 Torr = 133.3 Pa) was maintained during operation of the ESI source. In the cell, $[M + nH]^{n+}$ were *m/z*-selected by resonant frequency ejection techniques,²⁶ including correlated sweeps,²⁷ and were then allowed to react with reference compounds present at a static pressure of $(2-60) \times 10^{-8}$ Torr. Because ionic charge affects image current detection efficiency, all measured ion peak intensities were corrected for charge state before calculation of experimental rate constants. Reaction efficiencies are reported as the ratio of the experimental rate constant (k_{exp}) to the collision rate constant obtained via thermal capture rate (k_{cap}) calculations.^{28,29} Pressures were determined with a calibrated ionization gauge.³⁰

The peptides used in this study were obtained from Sigma (St Louis, MO, USA) and Bachem Bioscience (Philadelphia, PA, USA). The reference compounds were purchased from Aldrich (Milwaukee, WI, USA).

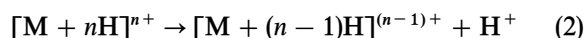
RESULTS AND DISCUSSION

The primary structures of the peptides studied are shown in Table 1. The three most basic amino acid residues and the *N*-terminal amino acid residue, which are likely protonation sites, are shown in capitalized and bold-faced text in the primary sequence in the table. These biomolecules contain a variety of amino acid residues and have differing sequences. For example, one of the peptides, ACTH (11-24), has six basic amino acid residues and contains a series of four adjacent basic residues, namely two lysine residues followed by two arginine residues. Another peptide, gastrin I (1-13), has only one intrinsically basic site, the *N*-terminal amino acid, and contains five adjacent glutamic acid residues. The remaining peptides examined in this study fall between these two extremes.

Table 2 contains the efficiencies for the reactions of $[M + nH]^{n+}$ from the seven peptides (M) studied with selected reference compounds (B) of known gas-phase basicity. The reaction monitored was



The Gibbs free energy, ΔG , for the deprotonation of $[M + nH]^{n+}$, as shown in the equation



is equal to the Gibbs gas-phase acidity:

$$GA([M + nH]^{n+}) = \Delta G \quad (3)$$

Owing to the reverse activation barrier (*RAB*) present in reaction (1), what is actually determined experimentally is the apparent gas-phase acidity, GA_{app} , as seen in the equation^{6,23-25}

$$GA_{app}([M + nH]^{n+}) = GA([M + nH]^{n+}) + RAB \\ \approx GB_{app}([M + (n-1)H]^{(n-1)+}) \quad (4)$$

The determined GA_{app} of each charge state is listed in Table 3. Note that a lower GA_{app} value means that an ion more readily donates a proton (i.e. is more acidic) and a higher value means that an ion more readily

Table 1. Small peptides involved in this study

Compound	Molar mass (Da)	No. of residues	No. of basic residues ^a	Max. No. of H ⁺ s added ^b	Sequence
ACTH (11–24) (human)	1652	14	6	5	LYS ¹ -Pro-Val-Gly- LYS ⁵ - LYS ⁶ - ARG ⁷ - ARG ⁸ -Pro-Val- LYS ¹¹ -Val-Tyr-Pro
Fibrinopeptide B (human)	1553	14	2	2	GLP ¹ -Gly-Val-Asn-Asp-Asn-Glu-Glu-Gly-Phe-Phe-Ser-Ala- ARG ¹⁴
Gastrin I (1–13) (human)	1706	14	1	2	GLP ¹ -Gly-Pro-Trp-Leu-Glu-Glu-Glu-Glu-Ala-Tyr-Gly-Trp
Renin substrate (horse)	1759	14	4	4	ASP ¹ - ARG ² -Val-Tyr-Ile- HIS ⁶ -Pro-Phe- HIS ⁹ -Leu-Leu-Val-Tyr-Ser
Somatostatin 14	1638	14	3	3	ALA ¹ -Gly-Cys- LYS ⁴ -Asn-Phe-Phe-Trp- LYS ⁹ -Thr-Phe-Thr-Ser-Cys
Substance P (synthetic)	1348	11	2	2	ARG ¹ -Pro- LYS ³ -Pro-Gln-Gln-Phe-Phe-Gly-Leu-Met-NH ₂
Tyrosine protein kinase (synthetic)	1593	13	3	3	ARG ¹ - ARG ² -Leu-Ile-Glu-Asp-Asn-Glu-Tyr-Thr-Ala- ARG ¹² -Gly

^a Basic residues refers to the number of arginine, lysine, histidine and *N*-terminal residues. If a lysine or arginine residue is located on the *N*-terminus, then it is counted as only one basic residue.

^b Maximum number of protons added by ESI for ions produced in greater than 10% intensity.

retains a proton (i.e. is more basic). As discussed previously by Zhang and Cassady,⁶ the assignment of GA_{app} is set at an efficiency of 0.10. The GA_{app} values include an uncertainty calculated from half of the difference in GB between the bracketing reference compounds at 0.10 efficiency plus an additional 2.0 kcal mol⁻¹ to account for uncertainties in the literature GBs of the reference compounds.

In Table 2, relatively low efficiencies are seen for several reactions with triethylamine and *N,N*-dimethyl-1,3-propanediamine. This effect is reproducible but the reason is unclear. Steric hindrance due to the size of the reference compound may be limiting access to the protonation site on the peptide. Steric hindrance has previously been observed to lower efficiencies for reactions involving various *tert*-butylated pyridine neutrals.³¹ This phenomenon could affect the correct assignment of the GA_{app} for $[M + 2H]^{2+}$ of tyrosine protein kinase (TPK).

For later reference, Table 4 lists the GBs of amino acids that may be serving as peptide protonation sites in the present study.

Charge state of $[M + 5H]^{5+}$

Of the peptides examined, only ACTH (11–24) readily attached five protons. Figure 1 shows a mass spectrum of the ACTH (11–24) ions as produced directly from the electrospray process. The peaks present in the figure correspond to $[M + nH]^{n+}$, $n = 2–5$. It should be noted that ACTH (11–24) contains a total of six intrinsically basic sites (Table 1), namely four lysine and two arginine residues (with one lysine as the *N*-terminal residue). The $[M + 6H]^{6+}$ ion was observed, but could not be isolated for reactivity studies owing to its very low intensity. Attachment of six protons to this bioactive tetradecapeptide represents protonation of 43% of the residues. This high degree of protonation is noteworthy, but it is not unprecedented. Downard and Biemann³² have observed a maximum protonation level of 42% for synthetic dodecapeptides containing arginine (by far the

most basic amino acid, see Table 4) and glycine residues.

The $[M + 5H]^{5+}$ ion was produced in large abundance and allowed to undergo deprotonation reactions with a series of reference compounds. If the five protons are attached to only the most intrinsically basic sites in the peptide, then significant Coulomb repulsion may exist in the ACTH (11–24) ions. This may be especially true if the most basic residues (Arg⁷ and Arg⁸) are both protonated. In this case, the most favorable sites of protonation may be at Lys¹, Lys⁵, Arg⁷, Arg⁸ and Lys¹¹ in order to maximize the distance between charge sites, but still retain them on the most basic residues. Although protonation on two adjacent residues might be expected to be unfavorable, the protons on the δ -guanido group of the arginine side chains are separated by 14 atoms. A recent study by Dongré *et al.*³³ employing surface-induced dissociation (SID) has shown evidence that adjacent arginine residues on a peptide can be protonated. Also, Downard and Biemann³² provided collision-induced dissociation (CID) results indicating

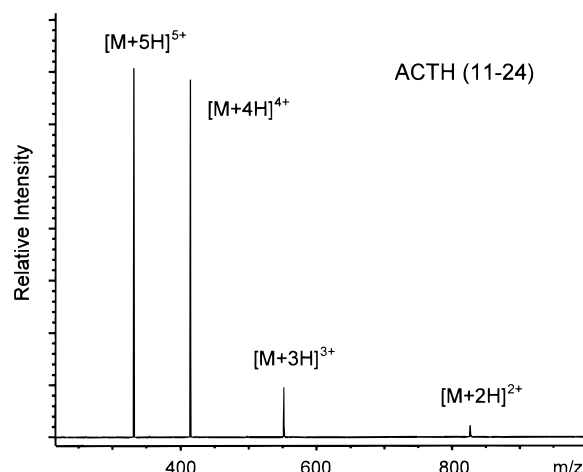


Figure 1. ESI-FT-ICR mass spectrum of ACTH (11–24) showing $[M + nH]^{n+}$, where $n = 2–5$.

Table 2. Reaction efficiencies for the deprotonation of small peptide ions, $[M + nH]^{n+}$

Peptide	<i>n</i>	Reference base (GB) ^a												
		MEA ^b 190.0	NH ₃ 195.6	2-CP ^b 200.3	2-FP ^b 202.8	3-FP ^b 206.2	NPA ^b 210.1	CHA ^b 213.4	DEA ^b 217.7	DPA ^b 219.7	TEA ^b 224.5	TPA ^b 226.2	DMPA ^b 229.4	TMDAB ^b 232.6
ACTH (11–24)	5	— ^d	0.007 ^c	0.244	0.462	0.193	0.736	0.269	0.420	0.677	0.587	0.754	0.332	0.818
ACTH (11–24)	4	—	0.000	0.004	0.004	0.109	0.502	0.605	0.483	0.755	0.290	0.680	0.459	0.760
ACTH (11–24)	3	—	—	—	—	—	0.001	0.010 (21%) ^e 0.070 (79%)	0.195	0.676	0.439	0.453	0.342	0.639
ACTH (11–24)	2	—	—	—	—	—	—	—	—	—	—	—	0.001	0.006 (26%) 0.071 (74%)
Fibrinopeptide B	2	—	—	—	—	—	0.000 ^f	0.022 ^f	0.350	0.627	0.161	0.585	0.708	0.720
Gastrin I	2	—	—	—	—	—	0.000 ^f	0.000 ^f	0.074 ^f	0.728	0.200 ^f	0.913	0.105	0.499
Renin substrate	4	0.000	0.170	0.342	0.400	0.479	0.510	0.587	0.636	1.099	0.469	0.718	0.889	0.746
Renin substrate	3	—	—	0.000	0.002	0.018	0.225	0.522	0.618	0.883	0.389	0.766	0.951	0.724
Renin substrate	2	—	—	—	—	—	0.000 ^f	0.000 ^f	0.000 ^f	0.135 ^f	0.150	0.323	0.841	0.417
Somatostatin	3	—	0.001	0.006	0.007 (30%) 0.034 (70%)	0.185	0.640	0.492	0.869	0.851	0.581	0.679	0.361	0.769
Somatostatin	2	—	—	—	—	—	0.009 ^f	0.030 ^f	0.066 ^f	0.118 ^f	0.228	0.138	0.021	0.543
Substance P	2	—	—	—	—	—	—	—	—	0.002 ^f	0.011	0.078	0.447	0.284
TPK	3	—	0.000	0.000	0.000	0.001	0.082	0.258	0.332	0.521	0.181	0.506	0.309	0.633
TPK	2	—	—	—	—	—	—	—	—	0.000 ^f	0.009	0.136	0.019	0.483

^a All GBs of reference compounds are from Ref. 46 and are given in kcal mol⁻¹.^b MEA = methyl acetate; 2-CP = 2-cyanopyridine; 2-FP = 2-fluoropyridine; 3-FP = 3-fluoropyridine; NPA = *n*-propylamine; CHA = cyclohexylamine; DEA = diethylamine; DPA = di-*n*-propylamine; TEA = triethylamine; TPA = tri-*n*-propylamine; DMPA = *N,N*-dimethyl-1,3-propanediamine; TMDAB = *N,N,N',N'*-tetramethyl-1,4-diaminobutane.^c Reaction efficiencies are the ratio of the experimental and theoretical rate constants: $k_{\text{exp}}/k_{\text{CAP}}$.^d Indicates that a reaction was not performed.^e In cases where an ion reacts at multiple rates, the percentage of the population reacting with each reaction efficiency is shown in parentheses.^f Adduct formation of the reference compound and peptide ion was observed.

Table 3. Apparent gas-phase acidities for the deprotonation of peptide ions $[M + nH]^{n+}$

Peptide	<i>n</i>	<i>m/z</i>	<i>GA_{app}</i> ^a (kcal mol ⁻¹)
ACTH (11–24)	5	331	197.4 ± 4.3
	4	414	205.9 ± 3.8
	3	552	215.5 ± 4.2 (20%) ^b 214.4 ± 4.2 (80%)
	2	827	>232.6 (25%) >232.6 (75%)
Fibrinopeptide B	2	777	214.4 ± 4.2
Gastrin I (1–13)	2	854	217.8 ± 3.0
Renin substrate	4	441	193.3 ± 4.8
	3	587	207.7 ± 4.0
	2	881	219.2 ± 3.0
Somatostatin 14	3	547	204.5 ± 3.8 (30%) 204.7 ± 3.8 (70%)
	2	820	219.0 ± 3.0
Substance P	2	675	226.4 ± 3.6
Tyrosine protein kinase	3	532	210.4 ± 3.6
	2	797	225.7 ± 2.8

^a All values are adjusted to the scale of Ref. 46. A lower *GA_{app}* value indicates that an ion is more acidic and a higher value that an ion is more basic.

^b In cases where multiple isomers were observed, the percentage of the ion population that has the listed *GA_{app}* is shown in parentheses.

the feasibility of adjacent sites of protonation. In comparison, a study employing a modified kinetic method on a series of doubly protonated nonapeptides showed no difference in either the *GB_{app}* or Coulomb repulsion, within experimental error, for terminal arginine residues (bradykinin, RPPGFSPFR) and adjacent arginine residues (RRPPGFSPF).²⁰

For $[M + nH]^{n+}$ from a *single* peptide, the facility of deprotonation increases as the charge state increases.^{5,7,34} However, our results indicate that a higher charge state peptide ion does not necessarily deprotonate before a lower charge state ion from *another* peptide of the same size. For example, both ACTH (11–24) and renin substrate have 14 amino acid residues, but the $[M + 4H]^{4+}$ of renin substrate is deprotonated more readily than $[M + 5H]^{5+}$ of ACTH (11–24). The major difference between the two peptides is the abundance of highly basic residues present in

ACTH (11–24). Not only are the composition and sequence of the two peptides different, but also the intramolecular interactions, such as intramolecular hydrogen bonding, between functional groups may differ. It has been shown previously that intramolecular hydrogen bonding can exist in singly charged small ions of peptides^{35–41} and amino acids,^{37,38,42,43} as well as larger multiply protonated peptide ions⁹; the result is an enhanced stability for the protonated ion. In particular, a recent study conducted in this laboratory suggests that the presence of intramolecular hydrogen bonding influences the basicities of di- and tripeptides containing lysine and histidine.⁴⁴ Peptides that contain a lysine residue generally have a higher GB than similar histidine-containing peptides.⁴⁴ This was attributed to the *n*-butylamine side-chain of lysine more readily forming intramolecular interactions than the imidazole ring side-chain of histidine. The presence of the above interactions could stabilize $[M + 5H]^{5+}$ of ACTH (11–24) and thus play a role in making this ion more difficult to deprotonate than renin substrate $[M + 4H]^{4+}$.

Comparison of $[M + 4H]^{4+}$

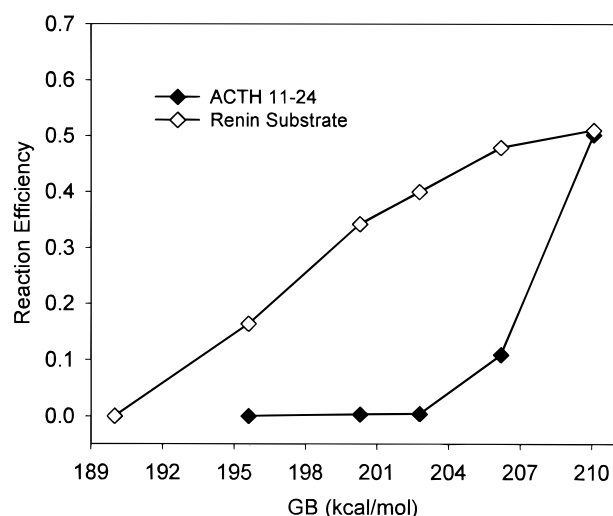
ACTH (11–24) and renin substrate were the only peptides studied that attached four protons. The reaction efficiencies of these two compounds are shown graphically in Fig. 2 as a function of the GB of the deprotonating neutral. In Fig. 2, and also in Figs 3 and 4, not all of the data points from Table 2 are plotted in order to reduce the complexity of the graphs. However, all data used in the *GA_{app}* assignments are included in the figures.

As seen in Fig. 2, the renin substrate $[M + 4H]^{4+}$ deprotonates more readily (i.e. has a lower *GA_{app}* value) than $[M + 4H]^{4+}$ of ACTH (11–24). Protonation of renin substrate probably occurs at the four intrinsically basic sites, which are Arg², His⁶, His⁹ and the *N*-terminal amino group of Asp¹. If the lysine and arginine residues are the sites of protonation on $[M + 4H]^{4+}$ of

Table 4. Gas-phase basicities of amino acids discussed in the text

Amino acid	<i>GB</i> ^a (kcal mol ⁻¹)	Ref.
Arginine	235.8	13
Lysine	220.8	44
Histidine	220.8	44
Tryptophan	217.6	46
Proline	213.3	41
Glutamine	210.6	46
Aspartic Acid	208.9	46
Glutamic Acid	208.7	46
Alanine	204.6	39
Glycine	201.4	48

^aAll values are adjusted to the scale of Ref. 46.

**Figure 2.** Reaction efficiencies for $[M + 4H]^{4+}$ versus gas-phase basicity of reference compounds.

ACTH (11–24), the Coulomb repulsions present may separate the protons as far as possible, such as Lys¹, Lys⁵, Arg⁷ or Arg⁸ and Lys¹¹. Alternatively, as stated above, protonation of adjacent arginine residues could exist and lead to placement of protons on Lys¹, Arg⁷, Arg⁸ and Lys¹¹. Examining all of the strong candidates for basic sites in these two peptides, the aspartic acid residue located on the *N*-terminus of renin substrate has by far the lowest intrinsic basicity and is expected to have the most easily removed proton. This is consistent with our experimental findings on the ease of deprotonation of renin substrate $[M + 4H]^{4+}$.

The data on $[M + 4H]^{4+}$ of ACTH (11–24) provide additional support for the conclusion that a protonated site's intrinsic acidity/basicity can sometimes be a more dominant factor than Coulomb repulsion in dictating the ease of deprotonation. Although it has a higher charge, $[M + 4H]^{4+}$ of ACTH (11–24) does not lose a proton as readily as $[M + 3H]^{3+}$ of somatostatin. For the somatostatin ions, protons may be removed from the low basicity *N*-terminal alanine residue while ACTH (11–24) ions would require the proton to be stripped from a considerably more basic lysine or arginine residue.

Comparison of $[M + 3H]^{3+}$

ACTH (11–24), renin substrate, somatostatin and TPK produced $[M + 3H]^{3+}$ directly from the electrospray process. The data on $[M + 3H]^{3+}$ reveal further selectivity in deprotonation reactions. Figure 3 shows that somatostatin $[M + 3H]^{3+}$ is the most readily deprotonated, followed by renin substrate, then TPK and finally ACTH (11–24) is the most difficult to deprotonate. As noted above, since somatostatin's three most basic sites include Ala¹, Lys⁴ and Arg⁹, the logical site for deprotonation would be the alanine residue owing to its low intrinsic basicity. In contrast, the $[M + 3H]^{3+}$ of renin substrate is probably protonated on Arg², His⁶ and His⁹ which have higher intrinsic basicities and therefore should not deprotonate as readily.

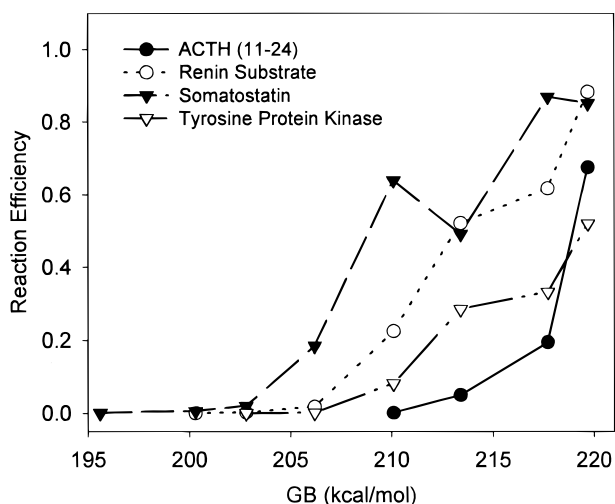


Figure 3. Reaction efficiencies for $[M + 3H]^{3+}$ versus gas-phase basicity of reference compounds.

The $[M + 3H]^{3+}$ of somatostatin showed non-linear pseudo-first-order kinetic behavior during deprotonation reactions with 2-fluoropyridine. (The somatostatin used in this study contained an intact disulfide (Cys³—Cys¹⁴) bond.) Similar behavior has previously been observed with other peptide ions and is an indication for the existence of structural isomers of $[M + nH]^{n+}$.^{1,5–7,9} Because our peptides were analyzed from a denaturing solution, the ions may be unfolded relative to their native structure; however, incomplete unfolding is also possible. As a result, isomers may be produced with different sites of protonation and/or different conformations. Evidence for structural isomers is generally only observed for thermoneutral deprotonation reactions. In each case here and in other studies in our laboratory^{1,6} the isomers were only seen when the reaction efficiency was below 0.10.

In examining the primary structures of ACTH (11–24) and TPK, the abundance of arginine residues stands out. TPK contains three (Arg¹, Arg², Arg¹²), whereas ACTH (11–24) has two (Arg⁷, Arg⁸) and four lysine residues. Since arginine is by far the most basic amino acid, protonated arginine residues should not readily lose a proton; in turn, this will increase the GA_{app} values of the peptide parent ions. Owing to its larger number of arginine residues, one might expect TPK to be more difficult to deprotonate than ACTH (11–24); in fact, the opposite trend is observed. Coulomb repulsion may be the major factor here. In particular, note that both peptides have adjacent arginine residues. TPK's options for protonation sites may be limited to its three arginine residues, yielding greater Coulomb repulsion and therefore increasing the facility with which a proton is lost from its $[M + 3H]^{3+}$. In contrast, ACTH (11–24) has multiple potential protonation sites that may allow the charge to be distributed to minimize Coulomb repulsion and maximize the stability of its $[M + 3H]^{3+}$. Also, the lysine residues within ACTH (11–24) can form extensive intramolecular hydrogen bonds adding to the stabilization of the protonation sites. For near thermal reactions, $[M + 3H]^{3+}$ and $[M + 2H]^{2+}$ of ACTH (11–24) also exhibited non-linear pseudo-first order kinetic behavior. This is evidence for two isomeric ion structures, which in this case may be due to differences in proton distribution among the six available basic sites.

Comparison of $[M + 2H]^{2+}$

All of the peptides would be expected to form $[M + 2H]^{2+}$ with the exception of gastrin I (1–13). This peptide contains a large number of adjacent glutamic acid residues but only one basic site, the *N*-terminal residue. However, gastrin I (1–13) also forms $[M + 2H]^{2+}$, as seen in the data in Table 2 and Figure 4. One proton may be located on the *N*-terminal pyroglutamate residue. However, the nitrogen of pyroglutamate is incorporated into an amide functionality, which should lower its basicity relative to that of an amine nitrogen. Recently, ion–molecule reactions with hydroiodic acid have suggested that the *N*-terminal pyroglutamate is not a basic site for multiply protonated neurotensin.⁴⁵ (Whereas the GBs of the 20 common

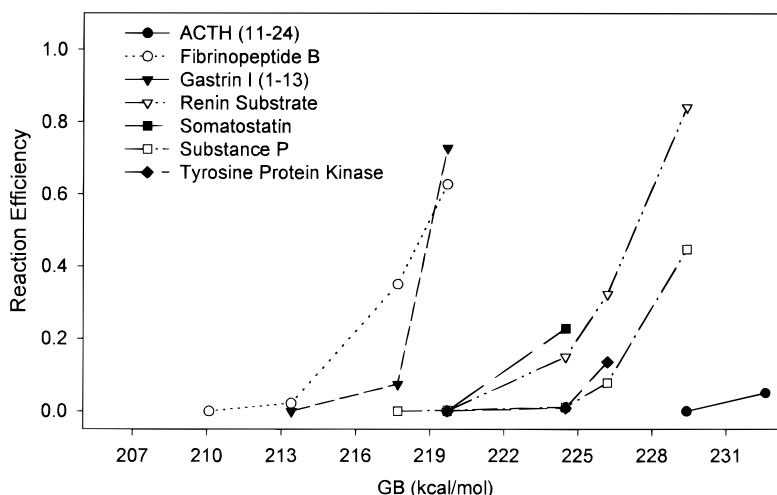


Figure 4. Reaction efficiencies for $[M + 2H]^{2+}$ versus gas-phase basicity (GB) of reference compounds.

α -amino acids have been measured, that of pyroglutamate is unknown; however, amides are known to have lower GBs than their primary amine counterparts.⁴⁶⁾ Other possible protonation sites for gastrin I (1–13) are Pro³, Trp⁴ and Trp¹². Molecular modeling studies by Schnier *et al.*¹⁶ have suggested proline, tryptophan and glutamine as protonation sites for ESI. Protonation along the carbonyl backbone is also conceivable.

The reaction efficiencies of $[M + 2H]^{2+}$ show fibrinopeptide B to be deprotonated most readily, followed by gastrin I (1–13). This trend is consistent with the trends in intrinsic basicity of the protonation sites. Fibrinopeptide B has several acidic residues (i.e. Asp⁵, Glu⁷ and Glu⁸), in addition to a basic residue at the C-terminus (Arg¹⁴) and a pyroglutamate residue at the N-terminus. The highly basic arginine residue should remain protonated in $[M + H]^+$ of fibrinopeptide B. With regard to the remaining potential protonation sites, the site on fibrinopeptide B (i.e. Glp¹) has a lower intrinsic basicity than those on gastrin (1–13) (i.e. Glp¹, Pro³, Trp⁴ and Trp¹⁴); consequently, fibrinopeptide B ions are deprotonated before the gastrin (1–13) ions. It should be noted that for ion production by ESI, the $[M + 2H]^{2+}$ of fibrinopeptide B and gastrin (1–13) were substantially less abundant than the $[M + 2H]^{2+}$ of the other peptides in this study. This could be attributed to lack of strong candidates for protonation sites on these acidic peptides in addition to the ESI conditions, such as source design, solvent composition and tuning parameters, that may discriminate against formation of $[M + H]^+$. (As is evident from Fig. 1, our ESI-FT-ICR system tends to favor the formation of higher charge state ions.)

Deprotonation reactions of renin substrate and somatostatin occur at equal efficiency within experimental error. For renin substrate, likely sites of protonation are Arg² and either His⁶ or His⁹. Somatostatin has basic residues at Lys⁴ and Lys⁹. This means that for both $[M + 2H]^{2+}$ the sites of the most easily removed proton are of near equal basicity (i.e. histidine and lysine).⁴⁴ Also, the charge sites are spaced at least four residues apart for each peptide. Thus, the presence of similar intrinsic basicities and minimal Coulomb repul-

sion is consistent with the $[M + 2H]^{2+}$ of renin substrate and somatostatin having near equal GA_{app} s.

Gross and Williams⁸ used deprotonation reactions to bracket the GA_{app} of gramicidin S $[M + 2H]^{2+}$ with a series of reference compounds (the literature values were reported as GB_{app} of $[M + H]^+$, which is essentially equal to the GA_{app} of $[M + 2H]^{2+}$). The GA_{app} was found to be 215.4 kcal mol⁻¹. Gramicidin S contains two ornithine residues separated by four residues in a cyclic decapeptide structure (*cyclo*[-PVOLF-]₂). Although the GB of the amino acid ornithine has not been determined, it differs in structure from lysine by only one less methylene group in its side-chain, that is, ornithine has an *n*-propylamino group where lysine has an *n*-butylamino group. Consequently, the GBs of these two individual amino acids should be similar at ~220.8 kcal mol⁻¹.⁴⁴ Somatostatin $[M + 2H]^{2+}$ contains two protonated lysine residues also separated by four residues and has a GA_{app} of 219.0 kcal mol⁻¹ which is in good agreement with the gramicidin S $[M + 2H]^{2+}$ data.

In contrast to renin substrate and somatostatin, basic sites on the other peptides are more closely spaced, namely, ACTH (11–24) has no separation between protonation sites of Arg⁷ and Arg⁸, substance P has one residue between Arg¹ and Lys³ and TPK has no separation between Arg¹ and Arg² or 10 residues between Arg¹ and Arg¹². Although these three peptide ions may experience greater Coulomb repulsion, they are all more difficult to deprotonate than the $[M + 2H]^{2+}$ of renin substrate and somatostatin. Hence the high intrinsic basicities of arginine and lysine are the dominant factor here in determining the GA_{app} . In particular, $[M + 2H]^{2+}$ for peptides containing two arginine residues were least susceptible to deprotonation; as a result, ACTH (11–24) and TPK ions have the highest GA_{app} values (i.e. are the most basic) of >232.6 and 225.7 kcal mol⁻¹, respectively. The GA_{app} values of ACTH (11–24) and TPK are in the same range as the GA_{app} of bradykinin $[M + 2H]^{2+}$, which was determined by a modified kinetic method to be 231.4 kcal mol⁻¹ (the literature values were reported as GB_{app} of $[M + H]^+$, which is essentially equal to the GA_{app} of

$[M + 2H]^{2+}$).²⁰ (Bradykinin (RPPGFSPFR) is a nine-residue peptide with an arginine residue on each terminus.)

The $[M + 2H]^{2+}$ of substance P deprotonated intermediate to the ions of TPK and ACTH (11–24). The protons on substance P are probably located at Arg¹ and Lys³. This peptide also contains three amide nitrogens (Gln⁵, Gln⁶, Met¹¹) that are capable of forming intramolecular hydrogen bonds with the long side chains of the protonated residues; this may contribute to the slight increase in GA_{app} of substance P ions over those of TPK.

The $[M + 2H]^{2+}$ ions possess similar mass-to-charge (m/z) ratios, but the GA_{app} values vary over a range of >18 kcal mol⁻¹. For larger peptides and proteins, we previously observed GA_{app} variations of <10 kcal mol⁻¹ for ions of similar m/z .⁶ The present study suggests that for smaller peptide ions, factors such as intrinsic basicity of protonation sites and charge site proximity are of greater importance in dictating GA_{app} .

For most of the peptides ions in the +2 charge state, adduct formation of the reference compound and peptide was observed as noted in Table 2. The number of reference compound molecules that attached varied from one to two depending on the peptide and its charge state. Adduct formation often occurred for near thermoneutral reactions and has also been reported in

previous studies with singly charged amino acid and peptide ions generated by FAB.^{38–40,44,48} Studies are in progress to explore the sites of these adduct attachments.

CONCLUSIONS

Seven small peptides of varying amino acid composition and sequence were analyzed by electrospray ionization in a Fourier transform ion resonance cyclotron mass spectrometer. Deprotonation reactions were used to obtain apparent gas-phase acidities for each peptide charge state that was formed (i.e. $[M + nH]^n+$, where $n > 1$). For these small peptides, intrinsic basicity of the protonation sites has a major impact on gas-phase reactions. The proximity of protonation sites is also of importance, affecting both Coulomb repulsion and intramolecular hydrogen bonding (i.e. conformation).

Acknowledgements

For financial support, the authors thank the National Institutes of Health (RO1-GM51384-01A1) and the Ohio Board of Regents Action Fund, Academic Challenge and Research Challenge Programs.

REFERENCES

1. C. J. Cassady and S. R. Carr, *J. Mass Spectrom.* **31**, 247 (1996).
2. D. Suckau, Y. Shi, S. C. Beu, M. W. Senko, J. P. Quinn, F. M. Wampler and F. W. McLafferty, *Proc. Natl. Acad. Sci. USA* **90**, 790 (1993).
3. J. L. Stephenson, Jr, and S. A. McLuckey, *J. Am. Chem. Soc.* **118**, 7390 (1996).
4. J. L. Stephenson, Jr, and S. A. McLuckey, *Anal. Chem.* **68**, 4026 (1996).
5. C. J. Cassady, J. Wronka, G. H. Kruppa and F. H. Laukien, *Rapid Commun. Mass Spectrom.* **8**, 394 (1994).
6. X. Zhang and C. J. Cassady, *J. Am. Soc. Mass Spectrom.* **7**, 1211 (1996).
7. D. S. Gross, P. D. Schnier, S. A. Rodriguez-Cruz, C. K. Fagerquist and E. R. Williams, *Proc. Natl. Acad. Sci. USA* **93**, 3143 (1996).
8. D. S. Gross and E. R. Williams, *J. Am. Chem. Soc.* **117**, 883 (1995).
9. P. D. Schnier, D. S. Gross and E. R. Williams, *J. Am. Chem. Soc.* **117**, 6747 (1995).
10. J. A. Loo, C. G. Edmonds, H. R. Udseth and R. D. Smith, *Anal. Chem.* **62**, 693 (1990).
11. S. K. Chowdhury, V. Katta and B. T. Chait, *J. Am. Chem. Soc.* **112**, 9012 (1990).
12. R. Guevremont, K. W. M. Siu, J. C. Y. Le Blanc and S. S. Berman, *J. Am. Soc. Mass Spectrom.* **3**, 216 (1992).
13. Z. Wu and C. Fenselau, *Rapid Commun. Mass Spectrom.* **6**, 403 (1992).
14. K. Isa, T. Omote and M. Amaya, *Org. Mass Spectrom.* **25**, 620 (1990).
15. G. Bojesen, *J. Am. Chem. Soc.* **109**, 5557 (1987).
16. P. D. Schnier, D. S. Gross and E. R. Williams, *J. Am. Soc. Mass Spectrom.* **6**, 1086 (1995).
17. R. R. Ogorzalek Loo and R. D. Smith, *J. Am. Soc. Mass Spectrom.* **5**, 207 (1994).
18. R. R. Ogorzalek Loo, J. A. Loo, H. R. Udseth, J. L. Fulton and R. D. Smith, *Rapid Commun. Mass Spectrom.* **6**, 159 (1992).
19. E. R. Williams, *J. Mass Spectrom.* **31**, 831 (1996).
20. I. A. Kaltashov, D. Fabris and C. C. Fenselau, *J. Phys. Chem.* **99**, 10046 (1995).
21. I. A. Kaltashov and C. C. Fenselau, *Rapid Commun. Mass Spectrom.* **10**, 857 (1996).
22. I. A. Kaltashov and C. C. Fenselau, *J. Am. Chem. Soc.* **117**, 9906 (1995).
23. S. Petrie, G. Javahery and D. K. Bohme, *Int. J. Mass Spectrom. Ion Processes* **124**, 145 (1993).
24. S. Petrie, G. Javahery, H. Wincel and D. K. Bohme, *J. Am. Chem. Soc.* **115**, 6290 (1993).
25. S. Gronert, *J. Am. Chem. Soc.* **118**, 3525 (1996).
26. M. B. Comisarow, V. Grassi and G. Parisod, *J. Chem. Phys.* **57**, 413 (1978).
27. A. J. R. Heck, L. J. de Koning, F. A. Pinkse and N. M. M. Nibbering, *Rapid Commun. Mass Spectrom.* **5**, 406 (1991).
28. T. Su and W. J. Chesnavich, *J. Chem. Phys.* **76**, 5183 (1982).
29. T. Su, *J. Chem. Phys.* **88**, 5355 (1988).
30. J. E. Bartmess and R. M. Georgiadis, *Vacuum* **33**, 149 (1983).
31. M. Meot-Ner and S. C. Smith, *J. Am. Chem. Soc.* **113**, 862 (1991).
32. K. M. Downard and K. Biemann, *Int. J. Mass Spectrom. Ion Processes* **148**, 191 (1995).
33. A. R. Dongré, J. L. Jones, A. Somogyi and V. H. Wysocki, *J. Am. Chem. Soc.* **118**, 8365 (1996).
34. S. A. McLuckey, G. J. Van Berkel and G. L. Glish, *J. Am. Chem. Soc.* **112**, 5668 (1990).
35. K. Zhang, C. J. Cassady and A. Chung-Phillips, *J. Am. Chem. Soc.* **116**, 11512 (1994).
36. X. Cheng, Z. Wu and C. Fenselau, *J. Am. Chem. Soc.* **115**, 4844 (1993).
37. J. Wu, E. Gard, J. Bregar, M. K. Green and C. B. Lebrilla, *J. Am. Chem. Soc.* **117**, 9900 (1995).
38. J. Wu and C. B. Lebrilla, *J. Am. Soc. Mass Spectrom.* **6**, 91 (1995).
39. C. J. Cassady, S. R. Carr, K. Zhang and A. Chung-Phillips, *J. Org. Chem.* **60**, 1704 (1995).
40. K. Zhang, D. M. Zimmerman, A. Chung-Phillips and C. J. Cassady, *J. Am. Chem. Soc.* **115**, 10812 (1993).
41. N. P. Ewing, X. Zhang and C. J. Cassady, *J. Mass Spectrom.* **31**, 1345 (1996).
42. A. A. Bliznyuk, H. F. Schaefer and I. J. Amster, *J. Am. Chem. Soc.* **115**, 5149 (1993).

43. S. Campbell, J. L. Beauchamp, M. Rempe and D. L. Lichtenberger, *Int. J. Mass Spectrom. Ion Processes* **117**, 83 (1992).
44. S. R. Carr and C. J. Cassady, *J. Am. Soc. Mass Spectrom.* **7**, 1203 (1996).
45. J. L. Stephenson, Jr, and S. A. McLuckey, *Anal. Chem.* **69**, 281 (1997).
46. S. G. Lias, J. F. Liebman and R. D. Levin, *J. Phys. Chem. Ref. Data* **13**, 696 (1984).
47. J. Wu and C. B. Lebrilla, *J. Am. Chem. Soc.* **115**, 3270 (1993).
48. J. W. McKiernan, C. E. A. Beltrame and C. J. Cassady, *J. Am. Soc. Mass Spectrom.* **5**, 718 (1994).